Two-Dimensional ESEEM Spectroscopy of Nitrogen Hyperfine Couplings in Methemerythrin and Azidomethemerythrin

Sergei A. Dikanov,*,†,‡,⊥ Roman M. Davydov,† Astrid Gräslund,§ and Michael K. Bowman†

Contribution from Macromolecular Structure & Dynamics, Environmental Molecular Sciences Laboratory, Pacific Northwest National Laboratory, Richland, Washington 99352, the Institute of Chemical Kinetics and Combustion, Russian Academy of Sciences, Novosibirsk 630090, Russia, and the Department of Biophysics, Stockholm University, S-106 91 Stockholm, Sweden

Received December 15, 1997

Abstract: The application of a two-dimensional ESEEM spectroscopy, known as HYSCORE, to the study of the hyperfine couplings from the nitrogens of histidine and azide ligands in mixed-valent states of methemerythrin and azidomethemerythrin produced by low-temperature (77 K) γ-irradiation is described. The HYSCORE spectra contain groups of well-separated cross-peaks from directly coordinated and remote histidine nitrogens, and from nitrogens of the azide ligand. The observation of cross-features correlating double-quantum transitions allows direct estimation of the hyperfine couplings from all coordinated histidine nitrogens of semimethemerythrin which vary between 5 and 15 MHz as well as their changes upon azide binding. The results obtained show that two-dimensional spectroscopy provides significantly more information compared to one-dimensional techniques for the characterization of the paramagnetic centers involving large numbers of magnetically nonequivalent nuclei. This work forms the basis for the application of two-dimensional ESEEM in conjunction with low-temperature reduction for the detailed characterization of nitrogen coordination in diiron centers in proteins of unknown crystal structure.

Introduction

Oxo-bridged dinuclear iron centers are a common structural component in the active sites of a number of proteins and enzymes with quite different functions such as hemerythrin (Hr), the R2 subunit of class 1 ribonucleotide reductase (R2), methane monooxygenase (MMO), and purple acid phosphatases.[1] The dinuclear iron site potentially has three oxidation states: diferric or met [Fe(III), Fe(III)]; mixed-valent or semimet [Fe(II), Fe(III)], and the fully reduced, deoxy [Fe(II), Fe(II)]. The mixed-valent form of diiron sites is paramagnetic with an $S = 1/2$ ground state resulting from antiferromagnetic coupling of an $S = 5/2$ ferric iron, Fe(III), and an $S = 2$ ferrous iron, Fe(II). Due to this property, EPR[1] and the related high-resolution techniques of ENDOR[2−4] and ESEEM[5] have been used to characterize the electronic structure of the mixed-valent form and the ligation of the dinuclear center in proteins and model complexes (Table 1). However, such research has been limited because the mixed-valent states are unstable and chemical reduction is generally an unproductive route for their generation. The diferric sites of R2, Hr, MMO hydroxylase, and synthetic model complexes were recently reported to be singly reduced efficiently in frozen solution at 77 K utilizing mobile electrons generated by γ-irradiation.[6−8] The characteristics of the EPR spectra of the mixed-valent state produced in this way differ from those of the mixed-valent state produced by standard chemical reduction in solution, because the reaction of the mobile electron with the diferric center generally retains the same coordination environment as the fully oxidized initial state due to the low mobility of the system at low temperature.

High-resolution EPR techniques were applied with great success to the study of the chemically reduced mixed-valent state in MMO.[2−4] The hyperfine couplings from nitrogens of both histidines directly coordinated to Fe(II) and Fe(III) were recently determined from ENDOR spectra of the mixed-valent state of MMO from *Methylococcus capsulatis*.[4] Additionally, an earlier ESEEM investigation reported lines assigned to the remote nitrogen of the Fe(III) histidine.[3] The diiron center of hemerythrin is coordinated by five histidine residues[9,10] rather than the two in MMO. Thus, the contribution of at least 10 nitrogens (five coordinated and five remote) might be expected

† Pacific Northwest National Laboratory.
‡ Russian Academy of Sciences.
§ Stockholm University.
⊥ Present address: Department of Chemistry, SUNY−Binghamton, Binghamton, New York 13902.

(1) (a) Vincent, J. B.; Olivier-Lilley, G. L.; Averill, B. A. *Chem. Rev.* **1990**, *90*, 1447. (b) Que, L., Jr.; True, A. E. In *Progress in Inorganic Chemistry: Bioinorganic Chemistry*; Lippard, S. J., Ed.; Wiley: New York, 1990; Vol. 38, p 97. (c) Feig, A. L.; Lippard, S. J. *Chem. Rev.* **1994**, *94*, 759. (d) Wilkins, P. C.; Wilkins, R. G. *Coord. Chem. Rev.* **1987**, *79*, 195.

(2) Hendrich, M. P.; Fox, B. G.; Anderson, K. K.; Debrunner, P. G.; Lipcomb, J. D. *J. Biol. Chem.* **1992**, *267*, 261.

(3) Doi, K.; McCracken, J.; Peisach, J.; Aisen, P. *J. Biol. Chem.* **1988**, *263*, 5757.

(4) DeRose, V. J.; Liu, K.; Lippard, S. J.; Hoffman, B. M. *J. Am. Chem. Soc.* **1996**, *118*, 121.

(5) Bender, C. J.; Rozenzweig, A. C.; Lippard, S. J.; Peisach, J. *J. Biol. Chem.* **1994**, *269*, 15993.

(6) DeWitt, J. J.; Bentsen, J. G.; Rozenzweig, A. C.; Hedman, B.; Green, J.; Pilkington, S.; Papaefthymiou, G. C.; Dalton, H.; Hodgson, K. O.; Lippard, S. J. *J. Am. Chem. Soc.* **1991**, *113*, 9219.

(7) (a) Davydov, R.; Kuprin, S.; Gräslund, A.; Ehrenberg, A. *J. Am. Chem. Soc.* **1994**, *116*, 11120. (b) Davydov, R. M.; Smieja, J.; Dikanov, S. A.; Zang, L.; Que, L., Jr.; Bowman, M. K. *Inorg. Chem.*, submitted.

(8) (a) Davydov, R. M.; Ménage, S.; Fontecave, M.; Gräslund, A.; Ehrenberg, A. *J. Biol. Inorg. Chem.* **1997**, *2*, 242. (b) Davydov, R. M.; Davydov, A.; Ingemarson, R.; Thelander, L.; Ehrenberg, A.; Gräslund, A. *Biochemistry* **1997**, *36*, 9093. (c) Davydov, A.; Davydov, R.; Gräslund, A.; Lipcomb, J. D.; Andersson, K. K. A. *J. Biol. Chem.* **1997**, *272*, 7022.

(9) (a) Stenkamp, R. E.; Sieker, L. C.; Jensen, L. H. *J. Am. Chem. Soc.* **1984**, *106*, 618. (b) Holmes, M. A.; Stenkamp, R. E. *J. Mol. Biol.* **1991**, *220*, 723. (c) Stenkamp, R. E. *Chem. Rev.* **1994**, *106*, 715.

(10) Sheriff, S.; Hendrickson, W. A.; Smith, J. L. *J. Mol. Biol.* **1987**, *197*, 273.

S0002-7863(97)04234-0 CCC: $15.00
Published on Web 06/27/1998

Table 1. ENDOR and ESEEM Determined Nitrogen Couplings in Mixed-Valent State F(II)−Fe(III) of Diiron Centers

methane monooxygenase hydroxylase component from *Methylosinus trichosporium* (Hendrich et al.[2])
ENDOR: $A_N = 13.6$ MHz, $P_N = 0.7$ MHz ($g_1 = 1.94$), assigned to the nitrogen coordinated to Fe(III); estimated coupling $A_N \leq 7$ MHz of nitrogen coordinated to Fe(II)
methane monooxygenase hydroxylase from *Methylococcus capsulatus* (Bender et al.[5])
ESEEM: $a_{iso} = 5.0$ MHz, $r_{eff} = 2.2$ Å, $K = 0.75$ MHz, $\eta = 0.3$, nitrogen coordinated to Fe(II); $a_{iso} = 0.8$ MHz, $r_{eff} = 3.2$ Å, $K = 0.45$ MHz, $\eta = 0.35$, remote nitrogen of histidine coordinated to Fe(III)
methane monooxygenase hydroxylase from *Methylococcus capsulatus* (DeRose et al.[4])
ENDOR: hyperfine tensor (15.7; 15.7; 21) MHz, nitrogen coordinated to Fe(III); hyperfine tensor (4.3; 5.0; 6.4) MHz, nitrogen coordinated to Fe(II)
pink uteroferrin (Doi et al.[3])
ENDOR: $A_N = 12.6$ MHz, $P_N = 0.7$ MHz ($g_1 = 1.94$)
semimethemerythrin sulfide (Hendrich et al.[2])
ENDOR: $A_N = 12.1$ MHz, $P_N = 0.7$ MHz ($g_1 = 1.88$)

in ENDOR and ESEEM spectra of semimetHr. Even more nitrogens surround the diiron cluster in semimetHrN_3^-. However, the only published ENDOR study of semimetHr sulfide reports just one nitrogen coupling.[2]

The present paper reports two-dimensional ESEEM (known as HYSCORE) studies of the hyperfine couplings from nitrogens in semimetHr and semimetHrN_3^- radiolytically reduced at 77 K. With the aid of orientation-selection and the increased resolution of 2D spectroscopy we are able to characterize and assign the hyperfine couplings of all coordinated histidine and azide nitrogens for a geometry very close to that of the parent diferric state.

Experimental Section

The preparation of the metHr and metHrN_3^- samples from the worm *Themiste zostericola* has been described elsewhere.[7] The samples containing about 1 mM protein, 50 mM Tris−HCl buffer (pH7.3−7.6), 100 mM KCl, and 50 vol % glycerol were irradiated by ^{60}Co γ-rays while immersed in liquid nitrogen at a nominal dose rate of 1.2 Mrad/h for 3−5 h.

Pulsed EPR experiments were performed with an X-band Bruker ESP-380E spectrometer with an MD-5 dielectric resonator. The length of a $\pi/2$ pulse was nominally 16 ns. Four-step phase cycles, +(0,0,0), −(0,π,0), −(π,0,0), +(π,π,0) in the three-pulse sequence[11] and +(0,0,0,0), −(0,0,0,π), +(0,0,π,0), −(0,0,π,π) in the four-pulse HYSCORE sequence,[12] were used to eliminate unwanted features from the echo envelopes. An Oxford Instrument CF935 helium cryostat was used for temperature variation and control. The spectra were recorded at 15 K. Spectral processing of three- and four-pulse two-dimensional ESEEM patterns was performed using Bruker 2D WIN-EPR software.

HYSCORE Spectroscopy. HYSCORE spectroscopy is based on the four-pulse, two-dimensional (2D) ESEEM experiment with a pulse sequence of $\pi/2-\tau-\pi/2-t_1-\pi-t_2-\pi/2-\tau-$echo.[13] The intensity of the inverted echo after the fourth pulse is measured as a function of t_1 and t_2 with constant τ. Such a 2D set of echo envelopes gives, after complex Fourier transformation, a 2D spectrum with equal resolution in each direction. The general advantage of two-dimensional techniques lies in the creation of non diagonal cross-peaks whose coordinates are nuclear frequencies from opposite electron spin manifolds. The HYSCORE technique is sensitive to the relative signs of the correlated frequencies and consequently experimental spectra usually are represented as two quadrants (++) and (+−) of the 2D Fourier transform.

For a nucleus of spin $I = 1$ (such as a nitrogen^{14}N), there are 3 nuclear frequencies in each electron spin manifold ($\nu_{\alpha i}$ and $\nu_{\beta j}$) and 18 possible correlation features ($\nu_{\alpha i}$,$\nu_{\beta j}$) between frequencies from different electron spin manifolds including two dq−dq correlations, eight dq−sq correlations, and eight sq−sq correlations (dq = double-quantum, sq = single-quantum). They may appear in both the (++) quadrant and the (+−) quadrant. Typically, only a subset of these features are visible in the experimental spectra because some have negligible intensity while others appear in only one of the two quadrants.[14]

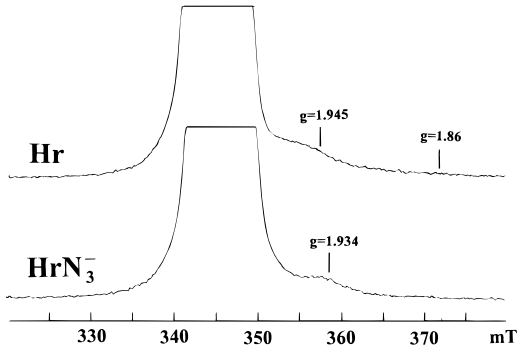

Figure 1. Field sweep two-pulse ESE spectra ($\tau = 240$ ns) of the irradiated methemerythrin and azidomethemerythrin frozen solutions. Microwave frequency 9.69 GHz.

The data available for coordinated histidine nitrogens in mixed-valent states of diiron clusters (Table 1), high-spin heme proteins,[15,16] and the reduced Rieske iron−sulfur center[17] (where two nitrogens coordinate the Fe(II) iron) uniformly show a nitrogen isotropic hyperfine constant of ≥4−5 MHz and a quadrupole coupling constant $K \approx 0.5-0.6$ MHz ($K = e^2qQ/4h$). For such a ratio of hyperfine and quadrupole couplings, one expects the most pronounced and easily recognized contribution to appear in the (+−) quadrant of X-band HYSCORE spectra from cross-peaks correlating two dq transitions from opposite manifolds.[14] Their assignment allows immediate estimation of the diagonal components of the hyperfine tensor in the **g** tensor coordinate system.

Results

The two-pulse, echo-detected EPR spectra of irradiated frozen solutions of metHr and metHrN_3^- are shown in Figure 1. The dominant contribution is from free radical signals near 345 mT with $g \approx 2$. This intense line overlaps an additional asymmetric feature at the high field edge of lower intensity with a maximum at 357−358 mT, corresponding to $g \approx 1.945$. Previous CW EPR studies reported that the mixed-valent state of the diiron center in irradiated frozen solutions of metHr and metHrN_3^- is characterized by an axial effective **g** tensor with principal values $g_\perp = 1.954$, $g_\| = 1.853$ (Hr), and $g_\perp = 1.944$, $g_\| = 1.923$ (HrN_3^-).[7,8] Therefore, the asymmetrical signal at the same region in the field-sweep ESE spectra is consistent with those

(11) Fauth, J.-M.; Schweiger, A.; Braunschweiler, L.; Forrer, J.; Ernst, R. R. *J. Magn. Reson.* **1986**, *66*, 74.
(12) Gemperle, C.; Aebli, G.; Schweiger, A.; Ernst, R. R. *J. Magn. Reson.* **1990**, *88*, 241.
(13) Höfer, P.; Grupp, A.; Nebenführ, H.; Mehring, M. *Chem. Phys. Lett.* **1986**, *132*, 279.
(14) Dikanov, S. A.; Xun, L.; Karpiel, A. B.; Tyryshkin, A. M.; Bowman, M. K. *J. Am. Chem. Soc.* **1996**, *118*, 8408.
(15) Scholes, C. P.; Lapidot, A.; Mascarenhas, R.; Inubushi, T.; Isaacson, R. A.; Feher, G. *J. Am. Chem. Soc.* **1982**, *104*, 2724.
(16) Jiang, Fa. S.; Zuberi, T. M.; Cornelius, J. B.; Clarkson, R. B.; Gennis, R. B.; Belford, R. L. *J. Am. Chem. Soc.* **1993**, *115*, 10293.
(17) (a) Gurbiel, R. J.; Doan, P. E.; Gassner, G. T.; Macke, T. J.; Case, D. A.; Ohnishi, T.; Fee, J. A.; Ballou, D. P.; Hoffman, B. M. *Biochemistry* **1996**, *35*, 7834. (b) Gurbiel, R. J.; Batie, C. J.; Sivaraja, M.; True, A. E.; Fee, J. A.; Hoffman, B. M.; Ballou, D. P. *Biochemistry* **1989**, *28*, 4861. (c) Gurbiel, R. J.; Ohnishi, T.; Robertson, D.; Daldal, F.; Hoffman, B. M. *Biochemistry* **1991**, *30*, 11579.

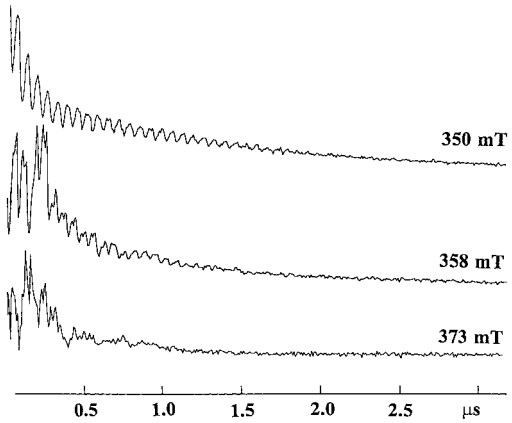

Figure 2. Two-pulse echo envelopes of the irradiated methemerethrin frozen solution at the magnetic fields 350 mT ($g = 1.98$), 357 mT ($g = 1.945$), and 373 mT ($g = 1.86$).

CW EPR observations and confirms that the mixed-valent state was trapped during irradiation.

ESEEM measurements at different field positions support this assignment (Figure 2). The two-pulse echo envelopes from the intense radical line (Figure 2, 350 mT) display only high-frequency modulation ~15 MHz corresponding to the proton Zeeman frequency and its second harmonic, indicating that protons are the only magnetic nuclei around the unpaired electron spins. The echo envelopes obtained between 355 and 373 mT ($g \approx 1.94-1.86$) show lower modulation frequencies with significant amplitude which we assign to the nitrogens in the diiron cluster. In practice, the partial overlap of the semimetHr and radical EPR spectra does not prevent the study of the nitrogen couplings in the reduced cluster because the radicals do not contribute to the nitrogen ESEEM. Similar results were obtained for the irradiated metHrN_3^- sample.

Semimethemerythrin. Three-Pulse Spectra. Parts a and b of Figure 3 show stacked plots of three-pulse ESEEM spectra recorded as a function of time τ at the high-field edge 373 mT ($g = 1.86$) of the Hr mixed-valent state EPR spectrum and at the maximum of its EPR signal 357 mT ($g = 1.945$). Measurements at different positions in the anisotropic EPR line select clusters with different orientations of the effective **g** tensor relative to the applied magnetic field.

The three-pulse spectra contain a peak at 15−16 MHz resulting from superhyperfine couplings of unpaired electron with surrounding protons. The contribution of free radicals to this proton peak is more significant at $g_\perp$ than at $g_\parallel$. The proton peak exceeds the intensities of nitrogen lines at $g_\perp$ which is closer to the radical line and became less intense in the spectrum recorded at high-field edge near $g_\parallel$.

In addition to the proton peak, a set of nitrogen lines in the region 0−12 MHz are present in both stacked plots. The orientation dependence of the nitrogen ESEEM is clearly seen. At the high-field edge, the narrow line at 9.6 MHz and two broad lines on 1.4−1.8 and 2.8 MHz dominate the spectrum. In contrast, at the maximum of the EPR line, two peaks at 2.7 and 6.2 MHz have the maximum intensity. Each spectrum also contains several lines of low intensity which are better resolved in the "single-crystal-like" spectrum at 373 mT.

HYSCORE Spectra near $g_\parallel$. The lines produced by the different nitrogens are correlated in HYSCORE spectra recorded near $g_\parallel$ and $g_\perp$. The spectrum obtained near $g_\parallel$, Figure 4a, exhibits all resolved correlation peaks that can be observed at this field. The three pairs of cross-peaks in the (+−) quadrant with coordinates at [±7.9; ∓3.8] MHz (N1), [±9.7; ∓5.4] MHz

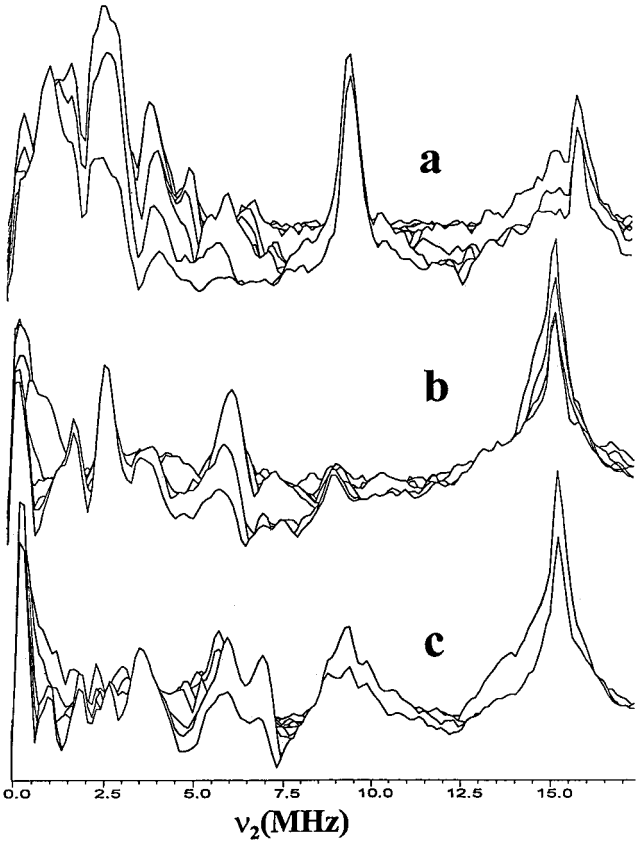

Figure 3. Superimposed plot of a set of three-pulse ESEEM spectra as the modulus Fourier transform along the T axis of semimethemerythrin recorded at the fields 373 mT ($g = 1.86$) (a) and 357 mT ($g = 1.945$) (b) and azidosemimethemerythrin recorded at the field 358 mT ($g = 1.94$) (c). The initial τ is 88 ns in the nearest trace, and by 16 ns in the successive traces.

(N2), and [±11.8; ∓7.3] MHz (N3) can be definitely assigned to dq−dq correlations of different nitrogens based on their frequency differences (close to $4\nu_I$ of nitrogen), their contour line shape, and their intensities.[14] (We use the notation [±7.9; ∓3.8] MHz to denote the pair of cross-peaks with coordinates (+7.9; −3.8) MHz and (+3.8; −7.9) MHz.) All other cross-peaks in the (+−) and (++) quadrants require more detailed scrutiny before assignment.

Nitrogen N1 is characterized by a set of well-pronounced peaks with dq transitions of 3.8 and 7.9 MHz. One can also assign to this nitrogen the cross-peaks [±7.9; ∓2.7] MHz (dq−sq correlation) and the [±4.8; ∓2.8] MHz (sq−sq correlation) and derive the two sets of nuclear frequencies as ~(7.9, 4.8, 3.1) MHz and ~(3.8, 2.7, 1.1) MHz assuming the same quadrupole contribution to the sq frequencies. The extended peaks around [5.0; 1.0] MHz with their typical orientation with respect to the diagonal are usually present for nitrogens with hyperfine coupling ~5 MHz and are interpreted as a sq−sq correlation for this nitrogen.[14] However, other nitrogens may also contribute to these extended peaks.

Both quadrants of the spectrum in Figure 4a contain cross-peaks at ~ [±9.7; ∓1.1] MHz, which correlate the dq transition 9.7 MHz of N2 with the sq frequency ~1.1 MHz from the same manifold with the 5.4 MHz dq transition. These cross-peaks together with the dq−dq correlations give first-order frequencies from the two opposite manifolds for N2 of ~(5.4, 4.3, 1.1) MHz and (9.7, 6.4, 3.2) MHz. This assignment is supported by weak cross-peaks at ~[6.2, 1.1] MHz in the (++) quadrant. After these considerations the intense peaks at ~[3.0; 1.1] MHz cannot

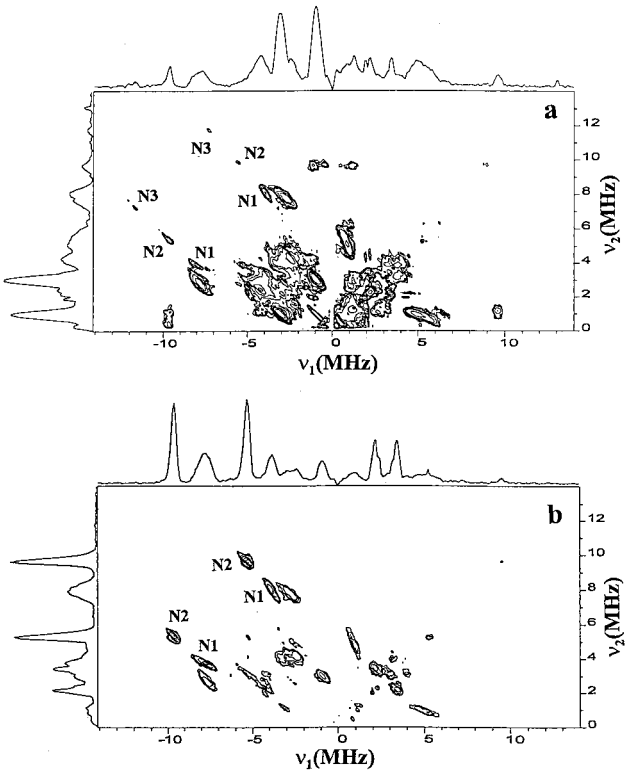

Figure 4. HYSCORE spectra of semimethemerythrin in the frequency range [±(0−14.0); (0−14.0)] MHz recorded at the field 373 mT (g = 1.86) and τ = 104 ns (a) and 136 ns (b).

be assigned to N1 or N2 alone. These peaks correlate the minimum sq frequencies from different manifolds which are equal in first-order for both nitrogens and, therefore, probably produced by N1 as well as N2.

The intensities of different cross-peaks are strongly affected by the value of τ as illustrated in Figure 4. For instance, the dq−dq correlations of N1 and N2 become stronger in the second spectrum. The weak dq−dq peaks of N3 at τ = 104 ns completely disappear at τ = 136 ns. However, they reach maximum intensity in the spectrum at τ = 200 ns (not shown) where the dq−dq peaks from N1 and N2 are not observed. There are no dq−sq correlations assignable to N3 with which to construct its nuclear frequencies. The intense features around the diagonals of both quadrants in the interval 0−5 MHz (Figure 4a) arise mainly from sq−sq correlations of coordinated as well as remote nitrogens. These features are nearly suppressed for larger τ although some regions show appreciable intensity. This τ dependence requires the collection of several HYSCORE spectra at each spectral position in order to observe all correlation peaks.

We estimate the diagonal elements of the nitrogen hyperfine tensor in the **g** tensor coordinate system using the formula based on the second-order expressions for the $\nu_{dq\pm}$ frequencies[18]

$$A_i = 2\nu_I(\nu_{dq+} + \nu_{dq-})/[8\nu_I - (\nu_{dq+} - \nu_{dq-})] \qquad (1)$$

The components of the hyperfine tensors for N1−N3 along the $g_{||}$ direction are given in Table 2.

HYSCORE Spectra near $g_\perp$. The dq−dq cross-peaks of N1 and N2 demonstrate more complex behavior in HYSCORE spectra recorded near $g_\perp$ at 357 mT (Figures 5a and 6a). The spectrum in Figure 5a (τ = 104 ns) shows intense peaks at

(18) Dikanov, S. A.; Tyryshkin, A. M.; Hüttermann, J., Bogumil, R.; Witzel, H. *J. Am. Chem. Soc.* **1995**, *117*, 4976.

Table 2. Frequencies of dq Cross-Features and Second-Order Corrected Hyperfine Couplings in SemimetHr

	dq cross-peaks (MHz)		hyperfine couplings (MHz)		
nitrogen	$g_{||}$	$g_\perp$	$A_{||}$	$A_\perp$	assignment
N1	[±7.9; ∓3.8]	[±7.6; ∓3.7]	5.3	5.0[a]	His73 (Fe(II))
N2	[±9.7; ∓5.3]	[±9.3; ∓5.2]	7.2	6.5[a]	His77,101 (Fe(II))
N3	[±11.7; ∓7.3]	[±11.6; ∓7.2]	9.1	9.4	His25 (Fe(III))
N4		[±17.4; ∓13.2]		15.3	His54 (Fe(III))

[a] Average value in $g_\perp$ plane.

Table 3. Frequencies of dq Cross-Features and Hyperfine Couplings in SemimetHrN_3^-

	dq cross-peaks (MHz)	hyperfine couplings (MHz)	
nitrogen	$g_\perp$	$A_\perp$	assignment
N1	[±7.6; ∓3.7]	5.1	His73 (Fe(II))
N2	[±9.3; ∓5.2]	6.7	His77,101 (Fe(II))
N3	[±9.9; ∓5.8]	7.3	His25 (Fe(III))
N4	[±17.0; ∓13.0]	15.0	His54 (Fe(III))
N_a	[±9.9; ∓5.8]	7.3	coordinated azide nitrogen
N_c	[4.6; 1.0]	∼2	central azide nitrogen

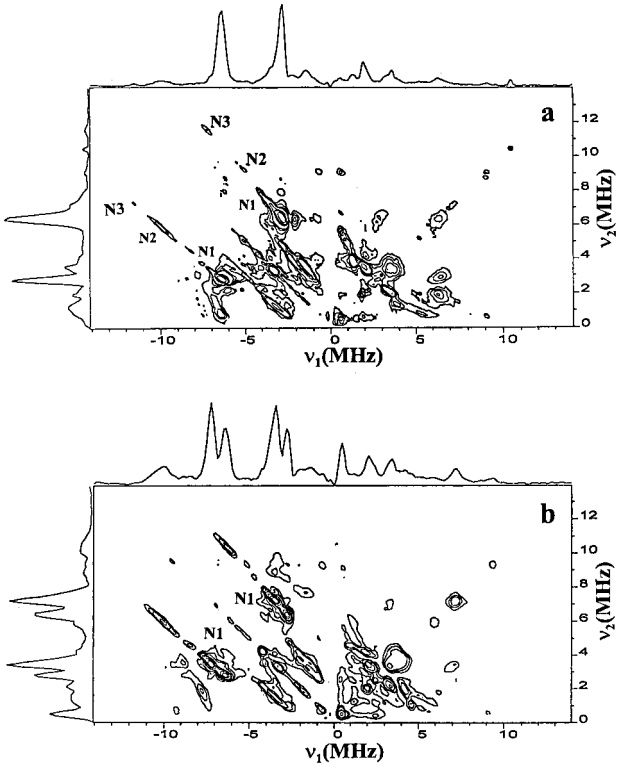

Figure 5. HYSCORE spectra of semimethemerythrin (a) and azidosemimethemerythrin (b) in the frequency range [±(0−14.0); (0−14.0)] MHz recorded at τ = 104 ns and the field 357 mT (g = 1.945) and 358 mT (g = 1.94), respectively.

[±6.4; ∓2.8] MHz with an asymmetric contour extending to the high-frequency direction along the diagonal. The most intense peaks are still at [±6.4; ∓2.8] MHz in Figure 6a (τ = 136 ns). However, they are accompanied now by narrow ridges centered at [±7.5; ∓3.7] MHz so that the complete features extend between 2.5−4.2 and 6.0−8.2 MHz in the two dimensions. These features are assigned to dq−dq correlations of N1. Such a long contour line shape results from a significant anisotropic hyperfine interaction which increases the spread of dq frequencies especially in the $g_\perp$ plane where many different orientations of the cluster relative to applied magnetic field are

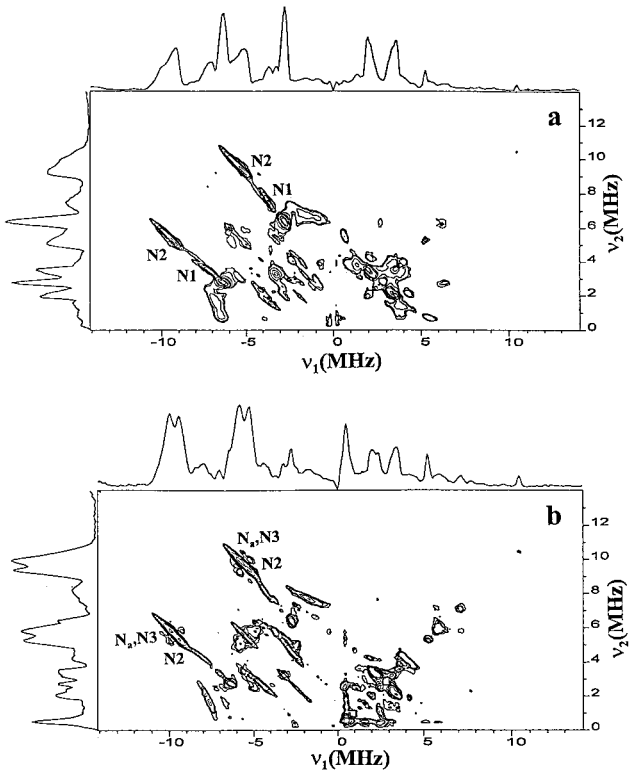

Figure 6. HYSCORE spectra of semimethemerythrin (a) and azidosemimethemerythrin (b) in the frequency range [±(0−14.0); (0−14.0)] MHz recorded at $\tau = 136$ ns and the field 357 mT ($g = 1.945$) and 358 mT ($g = 1.94$), respectively.

present. This assignment is confirmed by the simulations of HYSCORE spectra (see below). The separation between two points of these cross-peaks symmetrical relative to the diagonal slightly increases with increasing frequency in both dimensions from 3.5 to 4.0 MHz. It always remains less than $4\nu_I = 4.39$ MHz due to second-order contributions which vary for the different orientations. The contour line shape and distribution of intensities along the contour is determined by the principal values of the hyperfine and quadrupole tensors and their relative orientation. The application of eq 1 to the ends of the contour [±6.0; ∓2.5] MHz and [±8.2; ∓4.2] MHz gives hyperfine couplings ranging between 4.3 and 5.7 MHz in the $g_\perp$ plane with an average value of 5.0 MHz (Table 2).

A similar contour line shape is seen in Figure 6a consisting of two ridges of different intensity extended from 4.3 to 6.5 MHz and from 7.9 to 10.5 MHz. The lower frequency ridge has a low intensity while the high-frequency ridge has appreciable intensity and a pronounced maximum at [±9.3; ∓5.2] MHz. These features are assigned to N2. The estimated hyperfine couplings using eq 1 vary in the $g_\perp$ plane between 5.2 and 7.8 MHz with an average value of 6.5 MHz.

The lines at [±11.6; ∓7.3] MHz corresponding to features in the $g_\parallel$ spectra from N3 are also present in HYSCORE spectra at $g_\perp$ (Figure 7a). Weak cross-peaks at [±17.0; ∓12.6] MHz were also observed in some $g_\perp$ spectra which we assign to dq correlations of an additional nitrogen N4 (Figure 7a). We were unable to detect the corresponding peaks at $g_\parallel$ probably because of the lower signal-to-noise ratio in those spectra. Estimated hyperfine couplings using the frequencies at maximum intensity are 9.4 (N3) and 15.3 (N4) MHz.

In some $g_\perp$ spectra, another set of weak peaks at [∼±20; ∼∓12] MHz are seen (Figure 7b). We assign these peaks to double combination harmonics of the features at [±8.6−10.5; ∓4.7−6.5] MHz, indicating two nearly magnetically equivalent N2 nitrogens.

Simulations of HYSCORE Spectra. Generally, the analysis of the ESEEM and HYSCORE spectra recorded at canonical orientations of the axial **g** tensor presents an opportunity for the complete determination of nitrogen hyperfine and quadrupole tensors and their orientation in the **g** tensor coordinate system. However, all published analyses are for a single or a few magnetically equivalent nitrogens where all the nuclear frequencies and their combinations were clearly resolved and assigned. Such favorable conditions significantly limit the number of free fitting parameters and simplify spectral simulations. It seems very problematic to attempt this approach here because 10 parameters characterizing the principal components of the hyperfine and quadrupole tensors and their orientation need to be determined for each nitrogen and only limited information can be obtained from HYSCORE spectra due to overlap of more than 100 correlations in the frequency region [∼±5.0; ∼ ∓5.0] MHz. The features observed in HYSCORE spectra from nitrogen N1 and N2 do support quantitative analysis on an approximate level, which confirms assignments of the observed peaks and allows structural conclusions.

The nitrogen isotropic hyperfine coupling used in the simulations is based on second-order estimates from the experimental $g_\parallel$ and $g_\perp$ spectra (Table 2). In addition, published data for histidine-coordinated Fe(II) and Fe(III) in mixed-valent state,[4] Rieske-type iron−sulfur proteins[17] and heme proteins[15,16] give typical values for the anisotropic hyperfine tensor $T_\perp \sim -(1.0-1.5)$ MHz, and quadrupole couplings of $K = e^2qQ/4h \approx 0.5-0.6$ MHz, and asymmetry parameter $\eta \simeq 0.5 \pm 0.2$. The direction of the maximum principal axis of the quadrupole tensor lies close to the Fe−N bond direction.

The HYSCORE spectra recorded near $g_\parallel$ allow the first-order estimate of quadrupole splittings $Q_\parallel \approx 0.55$ MHz (N1) and 1.0 MHz (N2) along the $g_\parallel$ direction. The quadrupole splitting $Q_\parallel$ is[18]

$$Q_\parallel = K[(3 + \eta \cos 2\alpha)\sin^2 \beta - 2] \qquad (2)$$

with the orientation of the quadrupole tensor related to the effective **g** tensor axis by the Euler angles (α,β,γ). Using eq 2 with $K = 0.5-0.6$ MHz, one finds a quadrupole splitting ∼0.5 MHz for N1 at $\beta > 60°$ or $30° < \beta < 50°$ and ∼1 MHz for N2 at $\beta < 20°$ or $\beta > 70-90°$.

These ranges for the nitrogen tensors reproduce qualitatively (Figure 8) several important features in the HYSCORE spectra assigned to N1 for $\beta \approx 40-45°$. In the $g_\parallel$ spectra, dq−dq and dq−sq correlations (peaks 1 and 2 in the simulations) are close to each other, intense corrrelations in the low frequency region in (+−) quadrant (peaks 3) are present, and peaks 2 and espessially peaks 3 are suppressed when τ changes from 104 to 136 ns. In the $g_\perp$ spectra, peaks 2′ dominate for $\tau = 104$ ns and intense peaks 1′ and 3′ appear at $\tau = 136$ ns. All these features are reproduced simultaneously only when the axes of maximum principal values of hyperfine and quadrupole tensors are nearly coaxial (within 10−15°). The other four Euler angles have much less influence on the spectra. The simultaneous simulations of contour line shape show that peaks 1′ and 2′ do belong to the same dq−dq cross-feature, and can be definitely assigned to the same nitrogen (N1).

Simulations for N2 with similar conditions but different isotropic hyperfine constant reproduce the features definitely assigned to N2 for $\beta > 70°$. However, it must be noted that there is an additional complication because the peaks of N2 are produced by two approximately equivalent nitrogens with

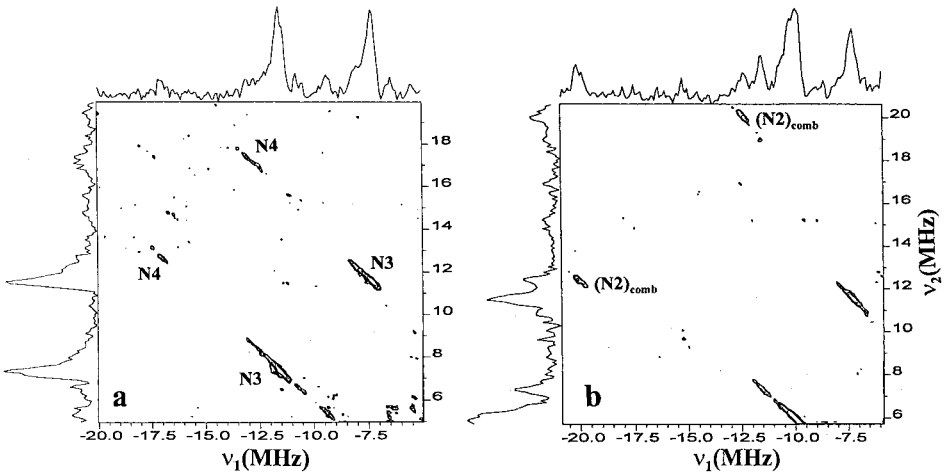

Figure 7. HYSCORE spectra of semimethemerythrin in the frequency range (a) [−(20.0−5); (5−20.0)] MHz recorded at $\tau = 200$ ns, and (b) [−(20.75−5.75); (5.75−20.75)] MHz, $\tau = 104$ ns. The field was 357 mT ($g = 1.945$) in both cases.

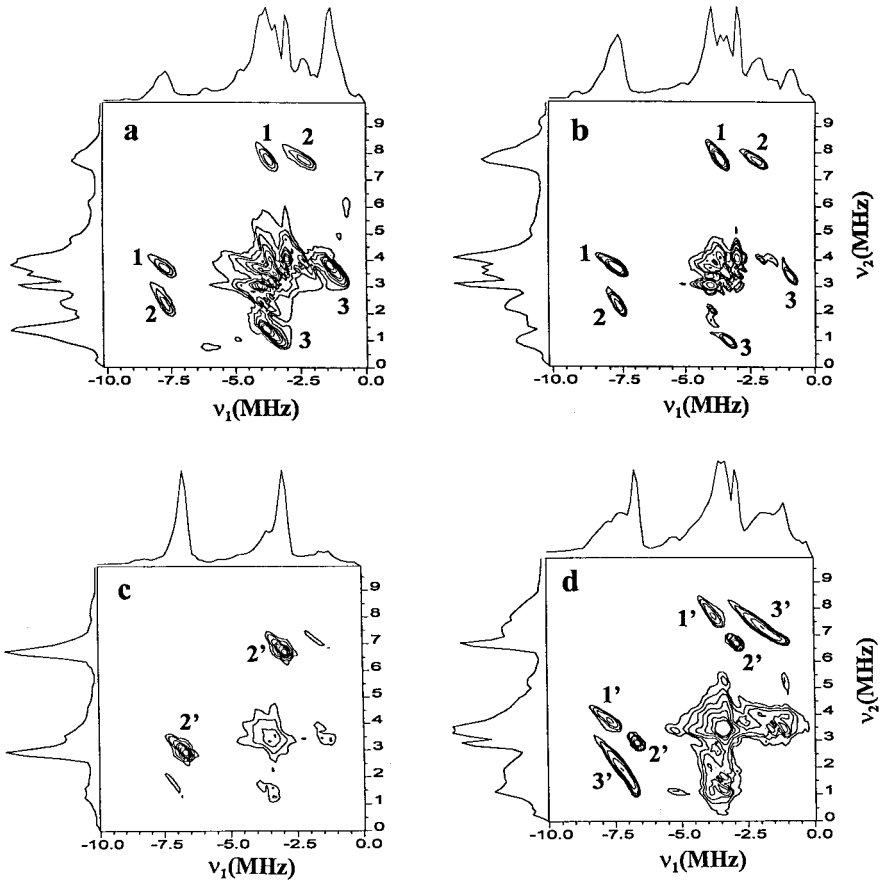

Figure 8. Simulation of the features assigned to N1 in experimental HYSCORE spectra: (a) $g_{||}$, $\tau = 104$ ns; (b) $g_{||}$, $\tau = 136$ ns; (c) $g_{\perp}$, $\tau = 104$ ns; (d) $g_{\perp}$, $\tau = 136$ ns. Parameters used in the simulations for shown spectra: $g_{\perp} = 1.954$, $g_{||} = 1.853$; nitrogen Zeeman frequency $\nu_I = 1.148$ MHz ($g_{||}$) and 1.0985 MHz ($g_{\perp}$); isotropic hyperfine constant 5.1 MHz; axial hyperfine tensor with perpendicular component $T = -1$ MHz; quadrupole coupling constant $K = 0.6$ MHz; asymmetry parameter $\eta = 0.5$. Angles between the unique axis of the **g** tensor and the maximal components of quadrupole $\beta = 40°$ and hyperfine $\theta = 45°$ tensors. All other Euler angles were chosen equal zero.

tensors having close but distinctly different orientations and principal values.

The observation of only the weak dq−dq correlations for N3 and N4 due to their decreased intensity with their larger hyperfine constant does not allow simulations for these nitrogen even at this approximate level. However, when such simulations are possible, they permit the correlation of observed hyperfine constants with the X-ray structure, particularly, for their assignment to histidine nitrogens.

Nitrogen Assignment. The X-ray crystal structures are available for azidomethemerythrin from *Themiste zostericola*[10] and for methemerythrin and azidomethemerythrin from *Themiste dyscrita*.[9] The comparison of the geometry of iron ligation in two azide complexes shows their high similarity with the differences in the angles between the corresponding iron−nitrogen and iron−oxygen bonds not more than several degrees only. It allows to suggest the similar ligation geometry of irons for metHr state in proteins from two sources because its structure

for *T. zostericola* is not available. Therefore, below we use X-ray structures of metHr and metHrN_3^- from *T. dyscrita*[9] as references for the analysis of HYSCORE data and for nitrogen assignment. There are five histidine residues, two carboxylic acid residues (Asp106 and Glu58), and a bridging oxygen bound to the iron atoms in hemerythrin. Three of the histidine residues (His73, 77, and 101) bind to iron Fe(1), and two (His 25 and 54) bind to the Fe(2). The six ligands of Fe(1) form an octahedron geometry with a slight distortion of 6−12° from 90° and 180° bond angles. The Fe(2) is pentacoordinated in a distorted trigonal bipyramid. The coordination of Fe(2) in the azidomet complex becomes octahedral with a larger distortion of as much as 26° for some angles.[9]

The mixed-valent state contains an $S = 5/2$ ferric iron, Fe(III), antiferromagnetically coupled to an $S = 2$ ferrous iron, Fe(II), to form an $S = 1/2$ electron spin state at low temperatures. The optical, Raman, and NMR spectroscopic studies indicate that the azide in semimetHrN_3^- is bound to the Fe(III) ion of the mixed-valent dinuclear center.[1b,19,20] The paramagnetic shifts and intensities of the N−H protons of imidazole residues in the NMR spectra of semimetHr and HrN_3^- is consistent with the Fe(II) center, i.e., Fe(1), coordinated to three His and the Fe(III) (Fe(2)), coordinated to two His and N_3^-. The absence of significant variations after azide binding in the cross-peak frequencies from the nitrogen with smaller couplings (see below) is also consistent with Fe(1) reduction in our sample.

According to the simple vector-coupling model, the antiferromagnetic coupling effectively scales the hyperfine tensors, *A*, of individual nitrogens as (7/3)*A* for nitrogens interacting with Fe(III) and (−4/3)*A* for nitrogens interacting with Fe(II).[21] Thus, we make an initial assignment of N1 and N2 (with two nuclei) as the three histidine nitrogens (His73, 77, and 101)[9] with the smallest hyperfine couplings coordinated to Fe(II). The angles between the Fe−N bonds of His73, 77, and 101 and the Fe−μ-O bond in the X-ray structure of metHr are 168°, 102°, and 97°, respectively, and the Fe(1)−μ-O−Fe(2) angle is 130°. The Fe−N bond of His73 forms an angle of ∼40° with the Fe(1)−Fe(2) direction, and the Fe−N bonds of His77 and 101 are nearly perpendicular to this direction. The angle β between the $g_{||}$ axis and the major principal axis of the quadrupole tensor obtained from simulations of HYSCORE spectra is 40−45° for N1 and >70° for N2 and would indicate that the $g_{||}$ axis is nearly collinear with the Fe(1)−Fe(2) direction and leads to the assignment of N1 to His73, and N2 to His77 and 101.

The remaining hyperfine couplings N3 and N4 involve the nitrogens of His25 and 54 coordinated to Fe(III). N4, with the larger hyperfine of ∼15 MHz, is assigned to His54 by analogy with the mixed-valent state of MMO where the nitrogen with the isotropic hyperfine coupling of ∼16 MHz involves a bond to Fe(III) approximately perpendicular to the Fe(II)−Fe(III) direction.[4] N3, with the coupling of ∼9 MHz, is assigned to His25. The Fe(III)−N vector for this histidine lies about 25° from the Fe(II)−Fe(III) direction.

Rescaling the average hyperfine couplings of N1 and N2 (5.0−5.3 and 6.5−7.2 MHz), assigned to the nitrogens coordinated to Fe(II), by a factor of 3/4 gives intrinsic coupling constants with absolute values of 3.75−4.0 and 4.9−5.4 MHz. The rescaled couplings for N3 and N4 (9.1−9.4 and ∼15 MHz) using 3/7 for Fe(III) have similar magnitudes of 3.9−4.0 and ∼6.4 MHz.

These rescaled constants for the nitrogens located axial to the Fe(II)-Fe(III) direction have a small coupling constant of ∼4 MHz while the nitrogens coordinated approximately perpendicular to this direction are larger, 5−6 MHz. This result may provide a simple indication of ligand geometry for diiron centers of unknown structure.

Azidosemimethemerythrin. ESEEM Spectra of Coordinated Nitrogens. The EPR spectrum of the irradiated frozen solution of metHrN_3^- is characterized by a significantly smaller **g** tensor anisotropy ($g_\perp = 1.944$, $g_{||} = 1.923$) compared to Hr ($g_\perp = 1.954$, $g_{||} = 1.853$).[7] Such small anisotropy prevents effective orientational selection at X-band or lower EPR frequencies, therefore, we consider just the spectra of semimetHrN_3^- obtained at the maximum of the EPR signal (358 mT, $g = 1.934$).

A set of spectral changes is clearly seen in the stacked plots of the three-pulse ESEEM spectra (Figure 3) after azide binding to the diiron center. The nitrogen ESEEM spectrum of semimetHrN_3^- no longer shows the intense pair of lines at 2.7 and 6.2 MHz which are replaced now by two peaks at ∼6.0 and ∼7.0 MHz and an asymmetric line at ∼3.5 MHz. Several unresolved lines with weak maxima at 8.8, 9.4, and 9.9 MHz are observed now in the frequency interval 7.5−12 MHz. All these spectral features have comparable intensity. The most intense line now appears at very low frequency. Oscillations corresponding to this frequency is clearly seen in the time-domain patterns. In addition, several weak maxima are present in the frequency intervals ∼1.0−3.5 MHz and 3.5−6.0 MHz. The spectral differences between semimetHr and semimetHrN_3^- may be associated with new contributions from azide nitrogens as well as with the different ligation geometry after azide binding accompanied by changes in electronic configuration and spin-density distribution over the diiron cluster.

HYSCORE spectra recorded for the same experimental conditions at the point of maximum EPR intensity of semimetHr and semimetHrN_3^- are shown in Figures 5 and 6. The HYSCORE spectra of semimetHr have maximum intensity at [±6.4; ∓2.8] MHz from the low-frequency part of N1 (His73) dq−dq correlation. The second part of this correlation with a maximum at [±7.6; ∓3.7] MHz is better seen in spectra recorded at larger τ values. The spectrum of semimetHrN_3^- recorded at $\tau = 104$ ns in contrast to the spectrum of semimetHr (Figure 5) shows both cross-features simultaneously with changed relative intensities. The [±7.6; ∓3.7] MHz peaks here increased relative to those at [±6.4; ∓2.8] MHz and now dominate the spectrum. This observation is consistent with the changes observed in the three-pulse spectra of semimetHr and semimetHrN_3^-.

The maxima of the dq−dq peaks from N2 remain practically at the same position [±9.3; ∓5.2] MHz after N_3^- binding but change in intensity and dominate in HYSCORE spectrum recorded at $\tau = 136$ ns (Figure 6b). Additionally, these peaks are accompanied by new, partially resolved cross-peaks at [±9.9; ∓5.8] MHz produced by the coordinated azide nitrogen. The application of eq 1 to the dq frequencies of 9.9 and 5.8 MHz estimates a hyperfine coupling for the coordinated azide nitrogen of 7.3 MHz.

We were unable to detect peaks near [±11.7; ∓7.3] MHz similar to the N3 peaks in Hr spectra. Therefore, we suggest that the hyperfine coupling of N3, (the coordinated nitrogen of His25) decreases after azide binding (from ∼9 to ∼7.3 MHz) and becomes similar to the coupling of the coordinated azide nitrogen. Both N3 and the coordinated azide nitrogen would produce cross-peaks at [±9.9; ∓5.8] MHz with intensities

(19) Irwin, M. J.; Duff, L. L.; Shriver, D. F.; Klotz, I. M. *Arch. Biochem. Biophys.* **1983**, *224*, 473.
(20) Maroney, M. J.; Kurtz, D. M., Jr.; Nocek, J. M.; Pearce, L. L.; Que, L., Jr. *J. Am. Chem. Soc.* **1986**, *108*, 6871.
(21) Sands, R. H.; Dunham, W. R. *Q. Rev. Biophys.* **1975**, *7*, 443.

comparable to those of the cross-peaks at [±9.3; ∓5.2] MHz from the two N2 nitrogens (His77 and His101). Thus, these two groups of nitrogens create doublets of equal intensity in Figure 6b.

The peaks from N4 in the spectra of semimetHrN_3^- are observed at practically the same frequencies [±17.0; ∓13.0] MHz, indicating that the hyperfine coupling of this nitrogen does not change significantly after azide binding.

We were unable to reproduce the experimental variation of line intensities from N1 and N2 after azide while binding keeping their positions invariant by simply changing the excitation conditions due to different **g** tensor principal values. According to the X-ray structure after the azide binding, the angle between Fe(III)−Fe(II) and Fe(II)−N for nitrogen N1 assigned to His 73 changes ∼9° from 39° to 30°,[9] producing a similar increase in the angle β if the orientation of quadrupole tensor is entirely determined by imidazole moiety. However, such minor variations of the angles between F(II)−Fe(III) and Fe−N do not lead to the experimentally observed results. The observed variations of intensity were reproduced qualitatively in simulations under the assumption that azide binding not only changes the principal values of the effective **g** tensor but also interchanges their principal axes also. That is, the axis of the minimal principal value is located in the plane of symmetry of two octahedrally coordinated irons after azide binding rather than along the Fe(II)−Fe(III) direction in semimetHr.

Low-temperature radiolytic reduction of the diiron center and the resultant trapping of the fully oxidized state in its nonequilibrium geometry prevent the use of wide temperature variations to determine the antiferromagnetic exchange coupling parameter *J*. Therefore, only continuous wave EPR microwave saturation measurements of *J* are available for radiolytically produced mixed-valent species, as well as the other data measured for chemically reduced species and model diiron model complexes.[7,8] They indicate values of $-J \leq 30$ cm^{-1}. $J = -13$ cm^{-1} was reported for the radiolytically reduced semimetHr[7] (with oxobridge) which is consistent with $J = -9$ cm^{-1} found for chemically reduced semimetHr[22] with the hydroxo bridge. Similary, a low $J = -7.6$ cm^{-1} was found for chemically reduced semimetHrN_3^-.[22] Such values of *J* are comparable to the zero-field splitting of ferrous iron Fe(II) in the five- and six-coordinated states $|D| < 12$ cm^{-1}, which mainly determines the **g** tensor anisotropy.[23]

At such low values of *J*, the components of the effective **g** tensor of the $S = 1/2$ ground state demonstrate a more complex dependence on *D* than the linear behavior predicted by the simple vector-coupling model. One of the possible results of such a dependence is the interchange of the order of $g_{\|}$ and $g_{\perp}$ which can occur even for small variations of *J* and *D* on the order of several cm^{-1} according to the analysis of McCormick et al.[22] Experimentally, the interchange of $g_{\|}$ and $g_{\perp}$ was observed by the same authors for two forms of semimetHr produced by the reduction of the metHr and oxidation of deoxyHr. This interchange was produced by the different sign of *D* in these two species.[22] The mixed-valent states produced by radialytic reduction in this work are characterized by significantly smaller **g** tensor anisotropy, so that even smaller differences in *J* or *D* between semimetHr and HrN_3^- may change the order of $g_{\|}$ and $g_{\perp}$ and the orientation of their axes.

Noncoordinated Azide Nitrogen. A completely new set of lines has appeared in the (++) quadrant of the HYSCORE spectra (Figures 5b and 6b) in the region 0−2.5 MHz, which we assign to a noncoordinated azide nitrogen. Two ridges at ∼0.5 MHz run parallel to the axes between ∼0.3 and 3 MHz. Their crossing at ∼0.5 MHz produces an intense diagonal peak. A peak at that frequency is the most intense feature in the three-pulse spectrum of semimetHrN_3^-. The extended straight ridge parallel to the axis indicates an absence of orientational dependence for the transition with the frequency 0.5 MHz. This is a characteristic of a pure quadrupole frequency in HYSCORE.[14] In paramagnetic systems such NQR frequencies appear when the hyperfine coupling approximately cancels the nitrogen Zeeman coupling in one manifold, i.e., when $\nu_I \simeq A/2$. This cancellation condition in one manifold also suggests that the frequency of the dq transition in the other manifold given by the approximate formula[24]

$$\nu_{dq+} = 2[(\nu_I + A/2)^2 + K^2(3 + \eta^2)]^{1/2} \qquad (3)$$

has to be $\geq 4\nu_I$ (which is 4.4 MHz) in the field 358 mT.

A careful inspection of HYSCORE spectra (Figures 5b and 6b) finds cross-features at ∼[1.0; 4.6] MHz which overlap other, weaker extended lines. These peaks together with the diagonal peak with short ridges at ∼1 MHz indicate the second quadrupole frequency is ∼1 MHz and the dq transition from the opposite manifold is ∼4.5−4.6 MHz. The quadrupole frequencies ∼0.5 and 1.0 MHz give $K = 0.25$ MHz and $\eta \approx 1$, which leads to dq frequency of 4.51 MHz corresponding to the frequency observed within experimental accuracy. An NMR study of KN_3 reports practically the same value of $K = 0.255$ MHz for the central nitrogen, and a larger value, $K = 0.45$ MHz, for the flanking nitrogens.[25] An even larger quadrupole coupling constant $K = 0.71$ MHz was reported for this nitrogen which coordinated the diiron center in the diferrous oxidation state.[26] We therefore assigned the new lines at low frequencies to the central azide nitrogen with $A \simeq 2$ MHz, $K = 0.25$ MHz, and $\eta \approx 1$.

Remote Nitrogens of Hisitidines. All HYSCORE spectra of semimetHr and semimetHrN_3^- contain prominent cross-peaks at [3.6; 1.9] MHz in the (++) quadrant. They have an asymmetric lineform seen in the skyline projections with a shoulder located closer to the diagonal which appears in some spectra as an additional weaker maximum. The sharpness of these lines, their intensity and location relative to the diagonal suggest that they are features correlating two formally double-quantum transitions, i.e., transitions between the extreme nuclear sublevels from opposite manifolds.

The remote nitrogen in the histidine rings is two additional bonds distant from the iron atoms and could produce these features. The hyperfine couplings of the remote nitrogen in model complexes of Cu^{2+} and $VO^{2+}$and in Cu^{2+}-proteins are about 10−20 times less than the coupling of the directly coordinated nitrogen.[27,28] An isotropic coupling of 0.8 MHz was found for the remote nitrogen of the histidine coordinated to Fe(III) in MMO[5] while the coupling for the coordinated nitrogen was $A = 13.0$ MHz.[2] The coupling of 0.36 MHz was found for the remote nitrogen of the histidine coordinated to

(22) McCormick, J. M.; Reem, R. C.; Solomon, E. I. *J. Am. Chem. Soc.* **1991**, *113*, 9066.
(23) Reem, R. C.; Solomon, E. I. *J. Am. Chem. Soc.* **1984**, *106*, 8323.
(24) Dikanov, S. A.; Tsvetkov, Yu. D.; Bowman, M. K.; Astashkin, A. V. *Chem. Phys. Lett.* **1982**, *90*, 149.
(25) Forman, R. A. *J. Chem. Phys.* **1966**, *45*, 1118.
(26) Sturgeon, B. E.; Doan, P. E.; Liu, K. E.; Burdi, D.; Tong, W. H.; Nocek, J. M.; Gupta, N.; Stubbe, J.; Kurtz, D. M., Jr.; Lippard, S. J.; Hoffman, B. M. *J. Am. Chem. Soc.* **1997**, *119*, 375.
(27) Mims, W. B.; Peisach, J. In *Advanced EPR. Applications in Biology and Biochemistry;* Hoff, A. J., Ed.; Elsevier: Amsterdam, 1989; p 1.
(28) Dikanov, S. A.; Samoilova, R. I.; Smieja, J. A.; Bowman, M. K. *J. Am. Chem. Soc.* **1995**, *117*, 10579.

Fe(II) in the Rieske center where the couplings of the coordinated nitrogens are about 5.0−5.5 MHz.[17a] These examples suggest that the couplings of the remote nitrogens of histidines around diiron center in semimetHr and semimetHrN_3^- should have values between 0.2 and 1.5 MHz.

The quadrupole coupling constant of the remote nitrogen measured in Zn^{2+}, Cd^{2+}, and Cu^{2+} model complexes with imidazole[27,29] and Cu^{2+}-proteins[27] demonstrate only a slight variation in quadrupole constant, $K = 0.35-0.43$ MHz, from the value of 0.35 MHz for the amine nitrogen in noncoordinated imidazole and histidine.[30] A similar value, $K = 0.45$ MHz, was reported for the remote nitrogen in MMO.[5] These considerations were used to select parameters for numerical simulation of HYSCORE spectra of a typical remote imidazole nitrogen in an iron complex. Using these parameters, we were able to simulate spectra with intense cross-peaks at frequencies close to the experimental ones at [3.5−3.9; 1.6−2.0] MHz for a broad range of the relative orientations of hyperfine and quadrupole tensors and for different τ values. These results allow us to assign these lines to the remote nitrogens of histidine. Their asymmetrical form probably results from the contribution of several nitrogens near the Fe(II) and Fe(III) whose average hyperfine couplings differ by a factor of nearly 2.

Conclusion

This paper describes the application of 2D ESEEM (HYSCORE) spectroscopy to the studying of the hyperfine couplings with the nitrogens of coordinated histidine and azide ligands in the paramagnetic, mixed-valent state of the diiron cluster Fe(II)−Fe(III) in semimetHr and HrN_3^- produced by γ-irradiation at 77 K. 2D spectra allow the observation of well-separated dq−dq cross-peaks from all coordinated histidine and azide nitrogens as well as additional lines from remote histidine nitrogens and the central azide nitrogen. The knowledge of both dq frequencies measured near the principal directions of the **g** tensor leads to a direct estimation of the diagonal components of the nitrogen hyperfine tensors and particularly the isotropic hyperfine constant. The isotropic hyperfine couplings for the nitrogens coordinated to Fe(II) are 5.2 and 7.0 MHz and 9.2 and ∼15 MHz for the nitrogens coordinated to Fe(III). The difference between these two sets of couplings is mainly caused by the difference in spin projection coefficients for Fe(II) and Fe(III). The rescaled isotropic couplings (3.9 and 5.25 MHz) for the nitrogens near Fe(II) are similar to those (3.9 and 6.4 MHz) for the nitrogens near Fe(III). The smaller constants belong to the nitrogens where the Fe−N bond is oriented close to the Fe(III)−Fe(II) direction and the larger ones to the nitrogens with Fe−N approximately normal to this direction. These results show that two-dimensional spectroscopy provides significantly higher resolution and more information compared to one-dimensional techniques and allows detailed characterization of paramagnetic centers surrounded by large numbers of magnetically nonequivalent nuclei (10 or 13 nitrogens in this particular case). This research provides a basis for the application of two-dimensional ESEEM in conjunction with low-temperature reduction for the characterization of nitrogen coordination in diiron centers of proteins with unknown structure.

There is another opportunity in the application of the 2D spectroscopy to the study of the mixed-valent states of diiron centers. The semimetHr and semimetHrN_3^- chemically reduced at room temperature have significantly larger **g** tensor anisotropy and a different temperature dependence when compared to the radiolytically produced semimetHr and semimetHrN_3^-. These differences result from transformation of the μ-oxo bridge in the metHr and metHrN_3^- precursors into a μ-hydroxo bridge when reduction is carried out at room temperature. 2D spectroscopy will make it possible to characterize the differences in nitrogen coordination between mixed-valent states with the geometry of the differic state as studied here with the equilibrium geometry of the mixed-valent state. This will allow characterization of changes that accompany cluster reduction at room temperature.

Acknowledgment. This work was sponsored by the U.S. Department of Energy under Contract DE-AC06-76RLO 1830 and by Associated Western Universities, Inc., Northwest Division (AWU NW), under Grant DE-FG06-89 ER-75522 or DE-FG06-92RL-12451 with the U.S. Department of Energy. S.A.D. acknowledges the receipt of a Faculty Fellowship from the AWU NW. R.M.D. is grateful for participation in the SABIT program.

JA9742343

(29) Ashby, C. I. H.; Cheng, C. P.; Brown, T. L. *J. Am. Chem. Soc.* **1978**, *100*, 6057.
(30) Hunt, M. J.; Mackay, A. L. *J. Magn. Reson.* **1976**, *22*, 295.